

# Chemical modification of polystyrene foam using functionalized chitosan with dithiocarbamate as an adsorbent for mercury removal from aqueous solutions

Babak Porkar\*, Pourya Alipour Atmianlu\*, Mahyar Mahdavi\*\*, Majid Baghdadi\*<sup>†</sup>,  
Hamidreza Farimaniraad\*, and Mohammad Ali Abdoli\*

\*Department of Environmental Engineering, Graduate Faculty of Environment, University of Tehran, Tehran, Iran

\*\*Department of Civil and Environmental Engineering, University of Nebraska, Lincoln, NE, 68588

(Received 21 August 2022 • Revised 27 November 2022 • Accepted 23 December 2022)

**Abstract**—One of the major environmental issues today is waste pollution, particularly non-biodegradable wastes such as polystyrene waste. Furthermore, heavy metal contamination is a major environmental threat. Mercury is one of the most hazardous and poisonous contaminants, and its usage in various industrial processes has resulted in contaminated effluents being released into surface runoff and groundwater. Because of the beneficial physical properties of polystyrene foam, this non-biodegradable waste was used in this study as a suitable medium for chemical modification. The polystyrene foam was first modified using crosslinked chitosan, and then it was reacted with carbon disulfide to improve its performance for the removal of  $Hg^{2+}$ . The prepared composite was used for the removal of mercury ions from contaminated water. The adsorbent's physical, chemical, and morphological properties were determined using energy-dispersive spectroscopy (EDS), Fourier-transform infrared spectroscopy (FT-IR), Field emission scanning electron microscopy (FE-SEM), and Brauer-Emmett-Teller (BET) analyses. Specific surface area, porosity, and average pore diameter were determined to be  $314.8\text{ m}^2/\text{g}$ ,  $0.345\text{ cm}^2/\text{g}$ , and  $1.96\text{ nm}$ , respectively. Experiments were designed to investigate the effects of pH, contact time, and contaminant concentration by the Box-Behnken response surface methodology. The maximum removal percentage of 79.85% was achieved for the initial mercury concentration of  $50\text{ mg/L}$  at pH 4. Moreover, the adsorption was observed to follow the Dubinin-Radushkevich isotherm. Studies on adsorbent recovery also showed that the adsorbent can be recovered and reused for at least three cycles.

Keywords: Mercury Removal, Water Treatment, Adsorption, Chitosan, Polystyrene

## INTRODUCTION

Heavy metal contamination in water poses a threat to the environment and is becoming a major health concern [1-3]. Mercury (Hg), which is one of the most hazardous heavy metals, biomagnifies through the food chain and can cause serious health problems [4]. Mercury contamination comes from human activities, including battery and electronic device manufacturing, smelting, fossil fuel combustion, and mining [5]. In the natural environment, mercury is primarily found in two forms: inorganic ionic form  $Hg(II)$  and organic form (methylmercury or ethyl mercury). Although organic mercury is more poisonous than inorganic ionic mercury due to its lipophilicity [6], inorganic  $Hg(II)$  is often found in natural aquatic environments and industrial wastewaters due to its high solubility and stability. Consequently, developing an effective method to remove  $Hg(II)$  from water is essential [7].

Over the years, various technologies for removing  $Hg(II)$  from water have been developed, including membrane filtration [8], coagulation [9], adsorption [10], flocculation [11], precipitation [12], and ion exchange [13]. Compared to other approaches, adsorption has been one of the most promising technologies for  $Hg(II)$  removal due to its low cost and ease of operation [14,15]. A variety of mate-

rials, such as activated carbon, chitosan, zeolite, and clay minerals, were used as adsorbents in the adsorption process [16].

Apart from heavy metal contamination, plastic waste pollution is the other major environmental concern. Polymers such as polyethylene (PE), polypropylene (PP), polystyrene, and polyethylene terephthalate (PET) constitute the majority of plastic waste. The fact that polymers are non-reactive is one of their advantages, but this feature makes plastic waste disposal difficult. For years, researchers have been looking for solutions to address the issue of plastic waste being disposed of in landfills. Upcycling plastic waste into valuable products is one of the most environmentally friendly solutions. For instance, it has been reported that synthetic polymers, specifically polyolefins such as polypropylene (PP) and polyethylene (PE), were used as oil sorbents [17-19]. Many studies have employed waste plastics for contaminant removal from water solutions. Janmohammadi et al. modified waste plastic filters for eliminating hexavalent chromium from electroplating wastewater [20].

Polystyrene is a styrene polymer that was discovered by a German chemist named Eduard Simon in 1839 through the distillation of liquid storax [17]. Polystyrene has attracted researchers' interest as a type of adsorbent because of its low cost, stable chemical properties, and strong hydrophobicity [21,22]. Polystyrene waste has been previously used for water and wastewater treatment purposes [23]. Pu et al. modified the waste polystyrene foam and applied it for the adsorption of organic dyes from water sources [24]. In this study, plastic waste was employed to fabricate polystyrene (PS)

<sup>†</sup>To whom correspondence should be addressed.

E-mail: m.baghdadi@ut.ac.ir

Copyright by The Korean Institute of Chemical Engineers.

granules for mercury removal from contaminated water [25,26].

Chitin is the second most abundant polysaccharide in the world, and its deacetylated derivative, chitosan, is a biocompatible, biodegradable, and non-toxic cationic polymer with amino and hydroxyl functional groups. Chitosan can be used in water treatment processes such as adsorption, chelation, precipitation, and ion exchange to remove toxic and hazardous pollutants [27,28]. Bionanocomposites composed of nanoparticles doped with chitosan have proven to be effective for removing contaminants from water [29,30]. Chitosan is more effective in the acidic medium as its amino functional groups can effectively be protonated in acidic media and bind with the anionic contaminants [31]. Physical modification has been attempted to improve the porosity and specific surface area of chitosan. Chitosan has also been combined with other materials (e.g., graphene, zeolite) to improve the adsorption performance of the resulting composite [16,32-34]. Chitosan modified with glutaraldehyde has been utilized for the removal of Rhodamine B dye [35,36].

Carbon disulfide is a colorless, volatile, inexpensive, and readily available chemical with numerous applications in organic chemistry [37,38]. A novel composite of carbon disulfide-modified magnetic ion-imprinted chitosan-Fe(III), i.e., MMIC-Fe(III) composite, was developed as an effective adsorbent for the simultaneous removal of tetracycline (TC) and Cd(II) [38].

Cross-linking is one of the most useful strategies to enhance the stability of chitosan inside an acidic medium, which improves its properties [39]. Glutaraldehyde has been reported as a chitosan cross-linking agent. It cross-links chitosan through bond formation between amino groups of chitosan and aldehyde groups of glutaraldehyde [40]. The type of functional groups of adsorbents has a considerable function in adsorbing heavy metals. As a result, the functionalization process can improve the performance of the adsorbent. In earlier studies, numerous functional groups, such as ethylenediamine, ethylenediaminetetraacetic acid (EDTA), thiourea, cysteine, citric acid, and  $\alpha$ -ketoglutaric acid, were incorporated into the structure of chitosan. Functional groups containing sulfur have a strong affinity for Hg(II). In this manner, Hg(II) can be successfully removed using sulfur-containing adsorbents without being affected by other most commonly coexisting hard cations and anions such as  $\text{Na}^+$ ,  $\text{Ca}^{2+}$ , and  $\text{Mg}^{2+}$  [41].

In this research, polystyrene waste was employed to synthesize an adsorbent for  $\text{Hg}^{2+}$  removal from contaminated water. First, the polystyrene foam was modified with crosslinked chitosan. Then it was chemically modified with carbon disulfide ( $\text{CS}_2$ ), incorporating dithiocarbamate functional groups. The modification of this plastic waste with chitosan and dithiocarbamate has not been reported in the literature. The modification of this plastic material with chitosan and dithiocarbamate can add high adsorption capacity to the composite. The adsorption process is highly influenced by the pH of the solution. The investigation of contact time is necessary to find the time at which the equilibrium of the adsorption occurs. The effect of pH, contact time, and initial mercury concentration was investigated to find out the optimum conditions for the adsorption of mercury ions by the prepared adsorbent. Experiments were designed by the Box-Behnken response surface methodology to investigate the effect of pH, contact time, and contaminant concentration. The isotherm, kinetics, and thermodynamics of the adsorp-

tion process were also investigated. The adsorption capacity of the prepared adsorbent was compared to other studies in the literature. The desorption and regeneration of the adsorbent were investigated to assess the capability of the adsorbent to be reused.

## MATERIALS AND METHOD

### 1. Reagents and Materials

The following materials were used for synthesis and analysis in this study: polystyrene foam as the adsorbent medium obtained from the recovery of plastic waste, chitosan, acetic acid ( $\text{CH}_3\text{COOH}$ ), sodium hydroxide (NaOH), glutaraldehyde (50%) ( $\text{C}_5\text{H}_8\text{O}_2$ ), ethanol ( $\text{C}_2\text{H}_5\text{OH}$ ), carbon disulfide ( $\text{CS}_2$ ), nitric acid ( $\text{HNO}_3$ ). The solutions of sodium hydroxide and sulfuric acid were used to adjust the pH of the solutions required for the tests. For evaluating the adsorbent performance in  $\text{Hg}^{2+}$  removal, 1,000 mg/L of mercury stock solution was prepared. The required stock solution was prepared by dissolving an appropriate amount of mercury (II) nitrate ( $\text{Hg}(\text{NO}_3)_2$ ) in 100 mL of distilled water. 0.5 mL of concentrated nitric acid (37%) ( $\text{HNO}_3$ ) was also added to the solution for the stabilization of mercury ions.

### 2. Instrumentation

Inductively coupled plasma-optical emission spectroscopy (ICP-OES) was used to determine the remaining mercury concentration in solutions. A pH meter (Behine, B2000 Model) was applied for adjusting the pH. FTIR analysis was performed by FTIR (Bruker). FESEM analysis was conducted by FESEM (MIRA3TESCAN-XMU). Other instruments included a magnetic stirrer (HS860 Model), oven (MODEL BM120), ultrasonic (PARSONIC 11s MODEL), and analytical balance (Ohaus MB35 Model).

### 3. Modification of Polystyrene Foam with Chitosan

The method used for the preparation of the polystyrene foam modified with chitosan was from a previous study [31]. First, the polystyrene foams were cleaned and separated to be ready for the next steps of adsorbent synthesis. Then, 1.25 g of chitosan was mixed with 50 mL of distilled water and 1 mL of acetic acid ( $\text{CH}_3\text{COOH}$ ) to obtain a solution for the modification of polystyrene foams. In the following, a sodium hydroxide solution was prepared by dissolving 15 g of NaOH in 35 mL of deionized water. The prepared polystyrene foam granules were immersed in chitosan solution and then removed after one to two seconds. Then they were immersed in the sodium hydroxide solution and removed immediately. The process of chitosan coating on granules was repeated. The granules modified with chitosan were allowed to remain in the sodium hydroxide solution for two hours. After two hours, the granules were removed from the sodium hydroxide solution and washed three times with distilled water.

### 4. Modification of Adsorbent with Glutaraldehyde and Carbon Disulfide

For further modification, granules coated with chitosan were treated with glutaraldehyde and carbon disulfide. For this purpose, 15 granules were placed in a beaker containing 50 mL of distilled water and 0.25 mL of glutaraldehyde ( $\text{C}_5\text{H}_8\text{O}_2$ ) for about one hour to achieve complete crosslinking. Then, the crosslinked granules were removed from the glutaraldehyde solution and washed twice with distilled water. After that, the granules were added to 25 mL

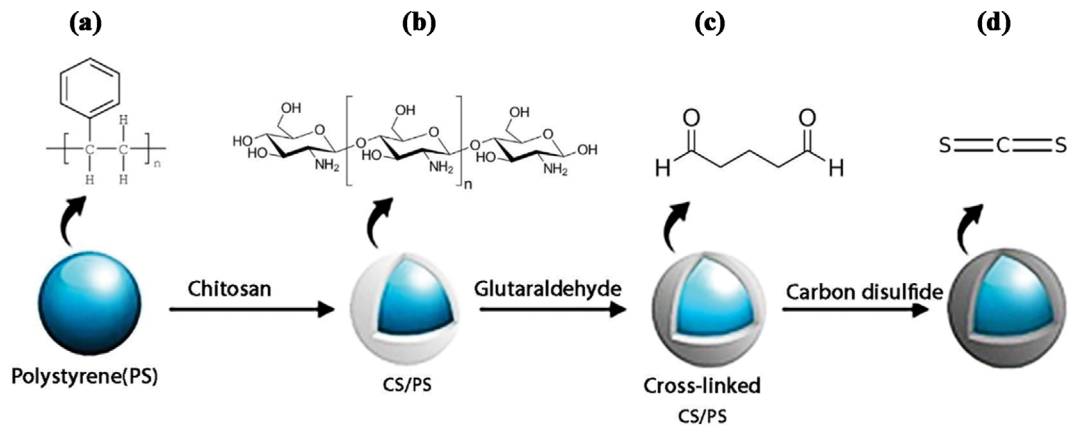


Fig. 1. Schematic presentation of polystyrene modification in different stages. (a) Foam without any modification, (b) Chitosan-modified granules, (c) Cross-linking of chitosan-modified granules with glutaraldehyde, (d) Dithiocarbamate functionalization of granules with carbon disulfide.

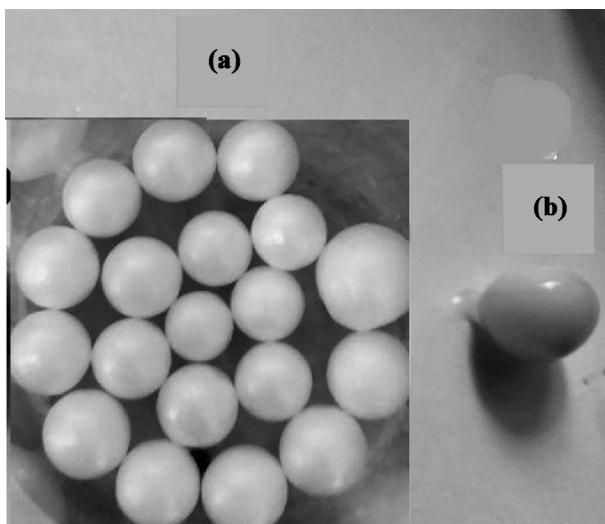


Fig. 2. Digital camera of (a) unmodified polystyrene granules, (b) Carbon disulfide-modified polystyrene granules.

of ethanol ( $C_2H_5OH$ ) and 1 mL of carbon disulfide ( $CS_2$ ), and the final mixture was shaken slowly for 30 min. Subsequently, the functionalized granules were washed with ethanol and distilled water twice to remove any excess material from the granules. Fig. 1 and 2 show the schematic presentation and digital camera of polystyrene modification in different stages, respectively.

### 5. Characterization

The infrared absorption spectra of chitosan-modified and dithiocarbamate-functionalized granules were determined using FTIR to identify the functional groups on the modified granules. To investigate the morphology of the prepared adsorbents, FE-SEM analysis was performed on chitosan-modified and dithiocarbamate-functionalized granules, and the results were compared with each other. Energy-dispersive spectroscopy (EDS) analysis was carried out on the prepared adsorbents to determine the weight percentage of different elements in the synthesized adsorbent before and after modification with carbon disulfide. The porosity and specific surface area

of the synthesized adsorbent were assessed using Brunauer-Emmett-Teller analysis.

### 6. Adsorption Studies

#### 6-1. Batch Experiment

Batch experiments were done to investigate the impact of various parameters on the adsorption process. The Box-Behnken design was employed for designing the experiments as it has the maximum performance for projects involving three factors and reduces the number of required experiments [42]. The volume of the wastewater solutions in the experiments was 50 mL. At the end of the experiments, the adsorbent was removed from the solution, and the remaining mercury concentration was determined by ICP-OES. The removal percentage and the adsorption capacity ( $q_e$ , mg/g) of the adsorbents were determined using Eq. (1) and Eq. (2). Solutions of NaOH and  $H_2SO_4$  (1 mol/L) were used to adjust the pH of the solutions.

$$\% \text{ removal} = \frac{C_i - C_e}{C_i} \times 100 \quad (1)$$

$C_i$  is the initial concentration of mercury in each solution, and  $C_e$  is the equilibrium concentration.

$$q_e = \frac{C_i - C_e}{W} \times V \quad (2)$$

In this equation,  $W$  is the weight of the adsorbent in grams, and  $V$  is the volume of mercury solution in liters.

#### 6-1-1. Effects of Various Parameters on the Adsorption Process

Design-Expert software was utilized to design experiments for evaluating the effects of pH, contact time, and initial mercury concentration. In these experiments, the range of different parameters was specified using the Box-Behnken response surface method. 17 experiments were designed with varying pH, adsorbent dose, contact time, and different initial mercury concentrations. Some preliminary tests were conducted to determine the range of the parameters for designing experiments. The pH range was between 2 to 6, the contact time was between 1 to 24 hours, and the initial concentration of the mercury was between 50 and 250 mg/L. For each experiment, the adsorbent was added to a beaker containing mer-

cury solution, and the pH of the solution was adjusted. The samples were mixed with a stirrer and then analyzed by ICP-OES to determine the remaining mercury concentration in the solutions.

#### 6-1-2. Study of Adsorption Isotherm

Designs performed by Design-Expert software have been used to study the adsorption isotherm. The removal efficiency was evaluated using the experimental formula derived from the Design Expert. Experimental conditions for these trials were as follows: 10 mL mercury solutions with initial concentration of 50 to 250 mg/L with steps of 20 and 30 mg/L, and an adsorbent weight of 0.0491 g. Adsorption isotherms at different pH levels (2, 3, 4, 5, and 6) were achieved.

#### 6-1-3. Desorption and Regeneration of the Adsorbent

To identify the rate of desorption, a hydrochloric acid solution (0.1 mol/L) was prepared. The adsorption process was performed with 50 mL of mercury solution with a concentration of 100 mg/L. After the adsorption and separation of the adsorbent, the desorp-

tion was carried out with 25 mL of the prepared hydrochloric acid solution. This experiment was repeated three times to assess the effectiveness of the adsorbent after washing with 0.1 mol/L hydrochloric acid solution. The time given for the adsorption process was 15 hours, and the time given for the desorption process was three hours.

## RESULTS AND DISCUSSION

### 1. Structural and Chemical Composition Characterization

FE-SEM analysis of the final adsorbent and the adsorbent before functionalization with carbon disulfide was performed to investigate the morphology of the adsorbent (Fig. 3). The morphology of the adsorbent differs before and after the sulfidation. Fig. 3 shows that the size of the pores has become smaller due to the reaction of chitosan with glutaraldehyde and carbon disulfide.

Fig. S1 shows the FTIR spectrum of the adsorbent in order to

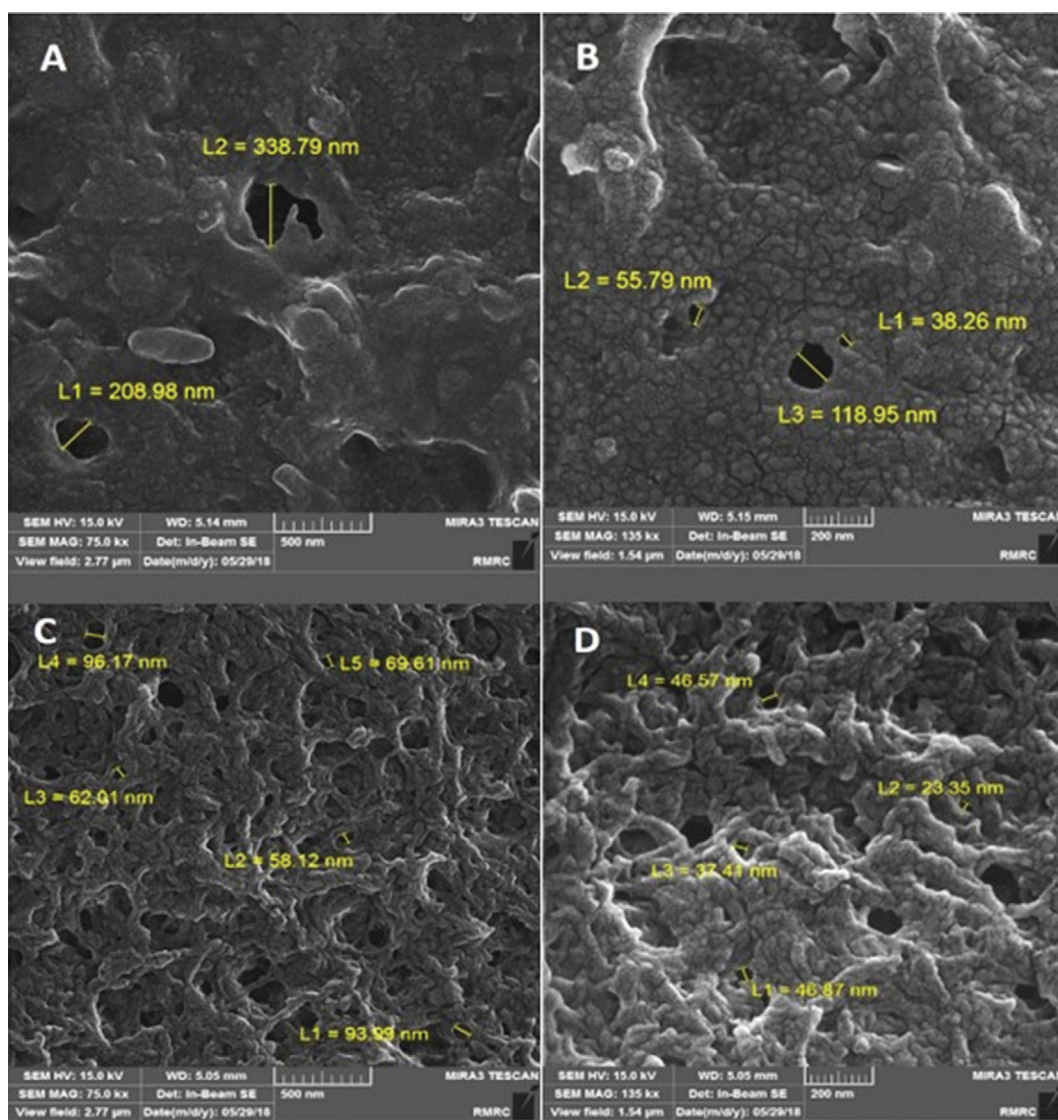


Fig. 3. The FE-SEM images of chitosan-modified granules (A and B) before the reaction with carbon disulfide, and (C and D) after the reaction with carbon disulfide.

**Table 1. EDS analysis of adsorbent before and after the reaction with carbon disulfide**

Element	Before the reaction with carbon disulfide (W%)	After the reaction with carbon disulfide (W%)
C	50.49	48.79
N	11.77	13.44
O	37.73	35.51
Na	-	0.97
S	-	1.29

identify the functional groups on the prepared adsorbent. Vibration of the hydroxyl groups was detected at  $3,393\text{ cm}^{-1}$  for the chitosan-modified adsorbent. Because the amine group in the functionalized chitosan was converted to NH, the peak at  $3,420\text{ cm}^{-1}$  corresponds to the vibrations of OH and NH bonds [43]. The intensification at the peak located at  $1,998\text{ cm}^{-1}$  also suggested an increase in amine groups. The peak at around  $1,080\text{ cm}^{-1}$  was due to the O-C bond of chitosan, whereas the peak at  $2,876\text{ cm}^{-1}$  was related to the  $\text{CH}_3$  bending mode [31]. The observed peak at  $1,650\text{ cm}^{-1}$  was most likely attributable to the vibration of the N-H bond [44].

EDS analysis (Table 1) was conducted to evaluate the weight percentage of different elements in the synthesized adsorbent before and after the treatment with carbon disulfide. Carbon, nitrogen, and oxygen are the main constituents of the adsorbent, with carbon being the most abundant constituent at about 50.49%, followed by oxygen at 11.77%. Sulfur was added to the adsorbent components due to the reaction with carbon disulfide. Sulfur is considered the main element for mercury adsorption in the adsorbent, and the weight percentage of sulfide in the final adsorbent was about 1.3%, which is an acceptable amount for mercury adsorption. The high

tendency of soft metals like mercury for interacting with the functional groups containing sulfur results in high adsorption of mercury by the prepared adsorbent. Therefore, the presence of sulfur in the adsorbent is the main factor in mercury removal in this study.

BET analysis is based on measuring the volume of nitrogen gas adsorbed and desorbed by the surface of the adsorbent at the temperature of liquid nitrogen (77 K). BET analysis indicates that the specific surface area, total pore volume, and mean pore diameter are respectively  $314.8\text{ m}^2/\text{g}$ ,  $0.345\text{ cm}^3/\text{g}$ , and  $1.96\text{ nm}$ .

## 2. Experimental Design

The Box-Behnken under Design-Expert was used to design the experiments. Table 2 shows the removal efficiency for each designed experiment. The proposed model was quadratic. ANOVA analysis was used to study the validation and significance of the parameters. Table 3 shows the ANOVA results derived from the Design Expert software. According to the ANOVA results, the F-static of 83.45 with a p-value of less than 0.0001 reveals the significance of the model [45]. Due to the p-value, which was 0.0001, it can be concluded that the model is suitable and is in line with the results. Lack of fit test was investigated, and the finding supported the quadratic model's agreement with the results. The correlation coefficient calculated with the following formula had a value of 0.9945. Adjusted R-Squared (0.9765) and predicted R-Squared (0.9560) values also confirmed the accuracy of the model. The effect of each parameter on the model was determined by p-values. If the p-value is less than 0.05, it implies that the parameter in the model is effective, and the parameter's significance increases as this value decrease. The p-value for pH was 0.0038, which determines the effect of pH on mercury removal. The contact time had a p-value of 0.0005, indicating that this factor had the most significant impact on mercury removal by the adsorbent. The initial concentration with the p-value of 0.0267 had the most negligible effect on mercury removal.

According to the definition provided for the p-value, the effect

**Table 2. Results from the designed experiments**

Experiment number	pH	Contact time (hr)	Initial mercury concentration ( $\text{mg L}^{-1}$ )	Removal efficiency (%)
1	4	12.5	150	74.6
2	6	24.0	150	69.8
3	6	12.5	250	70.9
4	6	1.0	150	7.7
5	6	12.5	250	61.0
6	4	12.5	150	77.9
7	4	12.5	150	77.4
8	2	24.0	150	58.6
9	4	12.5	150	71.6
10	2	12.5	50	68.7
11	4	1.0	250	7.7
12	4	24.0	50	79.9
13	4	1.0	50	10.4
14	4	12.5	150	72.6
15	2	12.5	250	51.8
16	4	24.0	250	56.3
17	2	1.0	150	7.6

Table 3. ANOVA for the quadratic model

Source	Sum of squares	df	Mean square	F-value	p-Value	Source
<b>Model</b>	11,888.81	8	1,486.10	83.45	<0.0001	Significant
A-pH	105.27	1	105.27	5.91	0.0411	
B-Time (hr)	6,675.90	1	6,675.90	374.87	<0.0001	
C-Hg (mg/L)	295.27	1	295.27	16.58	0.0036	
AB	29.38	1	29.38	1.65	0.2349	
AC	5.27	1	5.27	0.2958	0.6014	
BC	108.28	1	108.28	6.08	0.0390	
A <sup>2</sup>	127.88	1	127.88	7.18	0.0279	
B <sup>2</sup>	4,291.90	1	4,291.90	241.00	<0.0001	
<b>Residual</b>	142.47	8	17.81			
Lack of fit	63.31	3	21.10	1.33	0.3623	Not significant
Pure error	79.15	5	15.83			
<b>Cor total</b>	12,031.28	16				

of the interaction of different parameters on the whole adsorption process was also investigated. The pH-contact time interaction was the least effective, according to the observations, and the highest rate of interaction in the mercury removal process was found in the pH-initial mercury concentration. This software also developed the experimental equation for mercury removal, which was used to generate and study the adsorption isotherms (Eq. (3)).

$$\begin{aligned} \text{Removal (\%)} = & -20.80354 + (10.91072 * \text{pH}) + (9.07058 * \text{Time}) \\ & + (0.049212 * \text{Hg(II)}) + (0.11919) * \text{pH} * \text{Time} \\ & + (0.016972 * \text{pH} * \text{Hg(II)}) - (4.55967\text{E-}003 * \text{Time} * \text{Hg(II)}) \\ & - (1.65060 * \text{pH}^2) - (0.25406 * \text{Time}^2) - (3.97739\text{E-}004 * \text{Hg(II)}^2) \quad (3) \end{aligned}$$

### 3. Effect of pH, Contact Time, and Initial Mercury Concentration

The effects of pH, contact time, and initial concentration of mer-

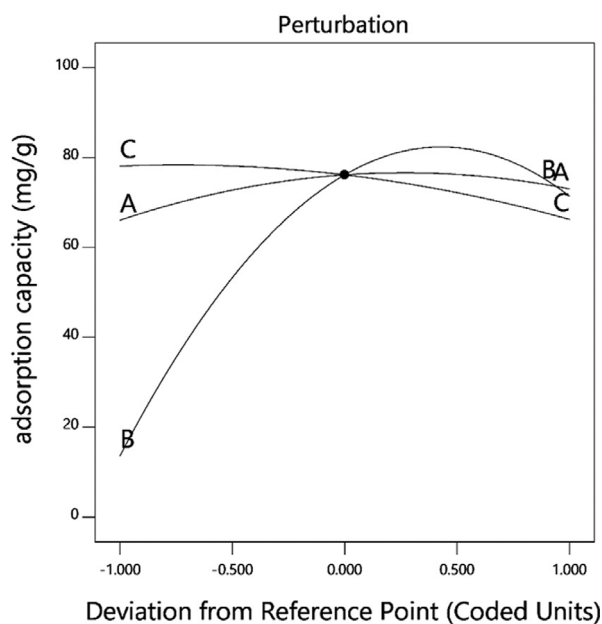


Fig. 4. Perturbation diagram, A: pH, B: contact time, and C: initial mercury concentration.

cury were studied because the adsorption process is highly dependent on these parameters. Fig. 4 shows the perturbation diagram, which is a graph that compares the effect of variables at specific points in the design space. This graph was drawn by changing each variable in a specified range and keeping the other variables constant. A high slope for a variable indicates that the results are susceptible to that variable. In Fig. 4, A is the pH, B is the contact time, and C is the initial mercury concentration. Due to the low slope of the curve related to the initial mercury concentration (C) and pH (A), these variables had the least effect on mercury removal, which was also confirmed by the ANOVA analysis. According to the slopes of the B curve, the contact time had a more significant effect on mercury removal.

The experimental results can be easily analyzed with the help of contour graphs and 3D interaction graphs of factors.

Fig. 5(a), (b), (e), and (f) showed that the removal efficiency increased with increasing the contact time. Then the increased trend slowed and eventually reversed after about 15 hours, probably due to the mercury desorption resulting from prolonged contact time. In the case of initial mercury concentration, Fig. 5(c), (d), (e), and (f) illustrate that the removal efficiency decreased slightly with increasing the initial mercury concentration. This behavior occurs because the available sites on the surface of the adsorbent are surrounded with more mercury ions, which results in decreasing mercury uptake. It is obvious that increasing the pH value results in higher removal efficiency. The zero point of charge ( $\text{pH}_{\text{zpc}}$ ) of the adsorbent was 5.1, which was measured using the procedure reported in the literature [46]. Furthermore, in pH values lower than the  $\text{pH}_{\text{zpc}}$  the adsorption occurs because of the complexation; however, in pH values over  $\text{pH}_{\text{zpc}}$  in addition to complexation, the electrostatic interaction because of the negative charge of the adsorbent can improve the removal efficiency [31]. There is an interaction observed in Fig. 5(e) between the initial mercury concentration and contact time, which shows that increasing the mercury concentration has a more significant impact on the process in higher contact times.

Since this study aims to maximize mercury removal efficiency, the goal "in range" was selected for the independent variables, and

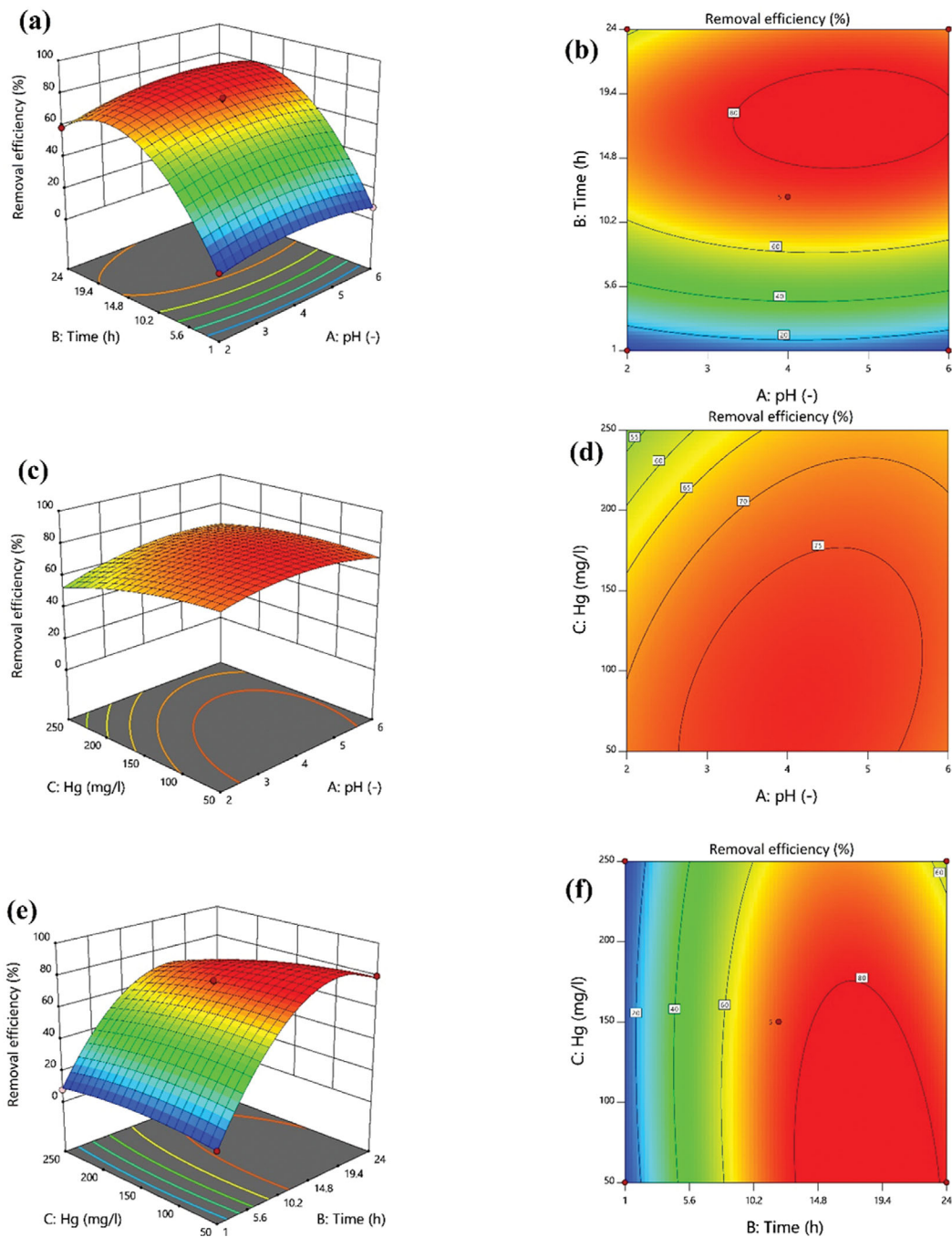


Fig. 5. 3D interaction graphs, (a) 3D graph of the effect of pH and contact time on the removal efficiency (initial concentration of mercury 150 mg/L), (b) 3D graph of the effect of pH, and initial mercury concentration on the removal efficiency (contact time 12.5 h), (c) 3D graph of the effect of contact time and initial mercury concentration on the removal efficiency (pH=4). The related contour plots are shown by (d), (e), and (f).

the “maximize goal was chosen for the response. Then, the optimization program was performed by the software, the result of which is given in Table 4. According to the optimum conditions reported in Table 4, the maximum removal percentage of 91.4% was achieved for the initial mercury concentration of 50 mg/L at pH 4.81 and 18.11 hr for the contact time. Desirability is a parameter derived from the design expert that represents the closeness of a response to its ideal value. The desirability of 0.92 shows that the response is

Table 4. Parameters for numerical optimization

Parameters	Value
pH	4.81
Time	18.11 hr
Initial concentration	50.0 mg/L
Removal percentage	91.4%
Desirability	0.92

**Table 5. Variables for different isotherms (contact time: 18 h)**

Isotherm	Equation	Variables	Values	R <sup>2</sup>
Freundlich	$C_e/q_e = 1/k_{qm} + C_e/q_m$	$K_f$	0.010	0.960
UT	$\ln\left(\frac{C_e}{q_e D} - \frac{K_d}{q_m D}\right) = -b \ln q_m + b \ln \frac{C_e}{D}$	$K_d$ (mg/L) $q_{max}$ (mg/g)	5.28 528	0.913
Redlich Peterson	$\ln\left(K_R \frac{C_e}{q_e} - 1\right) = \ln \alpha_R + g \ln C_e$	$\alpha$ $q_{max}$ (mg/g)	4.40 725	0.901
Dubinin-Radushkevich	$\ln q_e = \ln q_s - \beta \varepsilon^2$	$E$ (kJ/mol) $q_s$ (mg/g)	27.67 1,640	0.998
Temkin	$q_e = B_1 \ln A + B_1 \ln C_e$	$B_1$ (m/g) $A$ (L/mg)	1,090 0.028	0.987

92% close to the ideal value. However, the experiments for the adsorbent modified with glutaraldehyde without chitosan showed a mercury removal efficiency of 48% in the same optimum condition.

To validate the model, the experiment under the optimum conditions was conducted three times and the average response (89.4%) was in the proposed range (85.3-97.5%  $p=0.05$ ), showing that the model is valid.

#### 4. Adsorption Isotherms

The experimental formula generated by the Design Expert software was utilized to determine which isotherm is followed by the adsorption process. The adsorption capacity was calculated for various initial mercury concentrations, and adsorption isotherms were investigated based on these results. In this study, Freundlich, University of Tehran (UT), Redlich-Peterson, Dubinin-Radushkevich, and Temkin isotherms were used to examine the behavior of the adsorbent (adsorbent capacity, the ability for reducing the contaminant concentration, interaction strength) at the equilibrium state. The Langmuir constant represents the adsorption equilibrium constant. Using an adsorbent with a high Langmuir constant, a considerable reduction in the remaining concentration of the contaminant is attainable and the most active sites of the adsorbent are occupied. Therefore, a low amount of the adsorbent is used for water treatment. Table 5 shows the equations for each of the isotherms and the values for their variables.

In the case of Freundlich isotherm, the adsorption process oc-

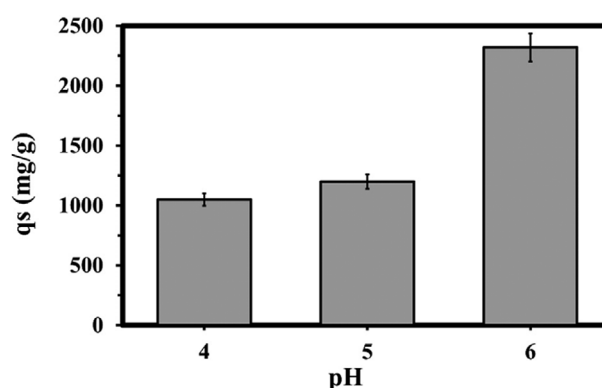


**Fig. 6.**  $q_s$  values for the Dubinin-Radushkevich model at different pH (The maximum adsorption capacity predicted in this isotherm was 2,449 mg/g at pH 6).

curs on a multilayer with the interaction between adsorbates. UT isotherm is a dose-independent isotherm with dimensionless parameters, which determines the multilayer maximum adsorption capacity that Freundlich isotherm is not capable of predicting [47]. The comparison between the studied isotherms was conducted according to the R-squared ( $R^2$ ) values obtained.

According to Table 5, the Dubinin-Radushkevich model was selected as the most suitable isotherm model for mercury removal

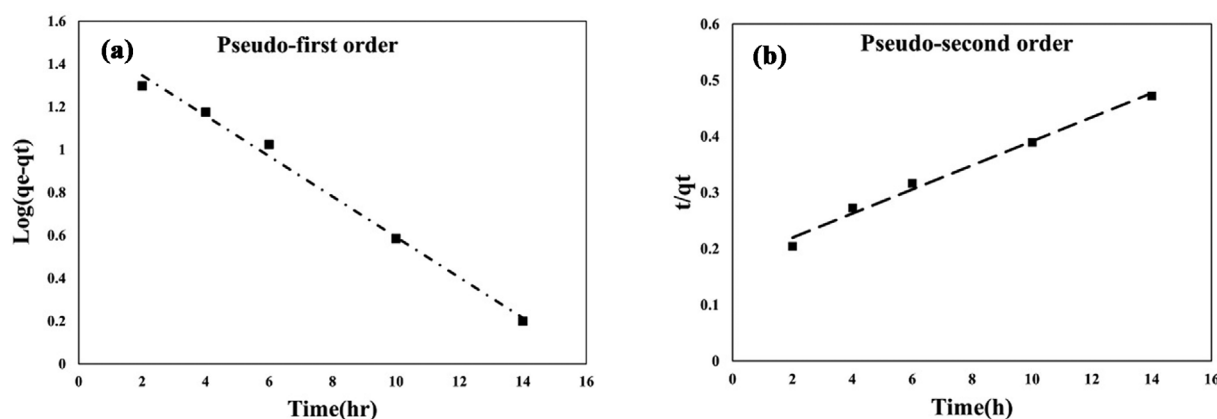


**Fig. 7.** Kinetic modeling of mercury adsorption (a) the pseudo-first-order, (b) pseudo-second-order models at the mercury concentration of 150 mg/L (Volume: 10 mL, adsorbent: 0.1 g).



**Table 6. Kinetics parameters and the error function values for the mercury adsorption**

Kinetics model	Parameters	$C_i=150$ (mg/L)
		$q_{exp}$ (mg/g)
Pseudo-first order	$q_e$ (mg/g)	27.83
$\text{Log}(q_e - q_t) = \text{Log}(q_e) - \frac{K_1 t}{2.303}$	$K_1$ (1/hr)	0.2
	RMSE	1.35
	$R^2$	0.99
Pseudo-second order	$q_e$ (mg/g)	22.04
$\frac{t}{q_t} = \frac{1}{K_2 q_e^2} + \left(\frac{1}{q_e}\right)t$	$K_2 \times 10^3 \left(\frac{g}{mg} \cdot \text{hr}\right)$	0.007
	RMSE	4.44
	$R^2$	0.98
Intraparticle diffusion $q_t = k_i t^{0.5} + C_i$	$k_i$	6.44
	$C_i$	0.11
	RMSE	1.1
	$R^2$	0.98

by the prepared adsorbent. The predicted  $q_e$  of the Dubinin-Radushkevich model and R-Squared were 1,640 mg/g and 0.998, respectively. When the adsorption energy ( $E$ ) is lower than 8 kJ/mol, the adsorption process can be classified as physical adsorption. Furthermore, when the adsorption can be classified as chemical adsorption when the adsorption energy is greater than 8 kJ/mol [48]. In this research, adsorption energy is 27.67 kJ/mol. Therefore, the adsorption can be classified as chemical adsorption. The maximum adsorption capacity for the Dubinin-Radushkevich model at various pH values was investigated and the results are shown in Fig. 6.

### 5. Kinetic Studies

A kinetic study was performed at mercury concentrations of 150 mg/L by pseudo-second-order and pseudo-first-order models. The corresponding linear plots and results are presented in Fig. 7 and Table 6, respectively. Among the investigated models, the pseudo-first-order model presented the lowest error function value ( $R^2=0.99$ , RMSE=1.35) than the pseudo-first-order model ( $R^2=0.98$ , RMSE=4.44). However, the pseudo-second-order model, in which the adsorption rate is proportional to the square of the number of free active sites, was significantly more accurate than the pseudo-first-order model because the equilibrium adsorption capacity calculated by the pseudo-first-order model was 27.83 mg/g, while the  $q_e$  calculated using the pseudo-second-order model was 22.04 mg/

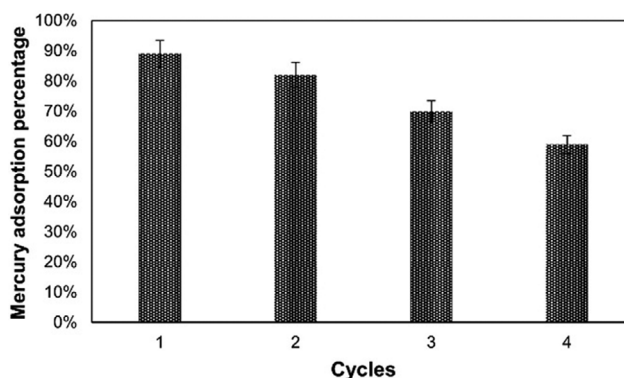


**Fig. 8. Reusability of the adsorbent after washing with 0.1 mol/L of HCl (Conditions: Sample volume: 50 mL, Desorption solution: 25 mL,  $Hg^{2+}$ : 100 mg/L, Adsorbent dosage: 1 g/L, Adsorption time: 12 h, and desorption time: 3 h).**

g, which was more consistent with the related experimental data.

### 6. Desorption and Regeneration of Adsorbent

To determine the efficiency of the adsorbent for reuse, the adsorption process was performed with 50 mL of mercury solution with a concentration of 100 mg/L and a contact time of 15 hours. Then,

**Table 7. Comparison of various adsorbents**

Type of adsorbent	The maximum adsorption capacity	Reference
FPBS	132.25	[49]
LCF wastes of coconut	144.4	[50]
PANI/ATP	800	[51]
CoFe <sub>2</sub> O <sub>4</sub> -RGO	140.84	[52]
Polystyrene@chitosan/dithiocarbamate	1,058	This study

the adsorbent was washed with 0.1 mol/L of hydrochloric acid. The adsorption process was repeated for four cycles with the same adsorbent and experimental conditions. Fig. 8 shows the mercury removal percentage for each cycle. The removal rate of mercury adsorption with the mentioned conditions in the first cycle was 89% and then it declined by 7%, 19%, and 40% for the second, third, and fourth cycles, respectively. Therefore, it can be concluded that the prepared adsorbent has the capability to be reused up to three times in order to achieve a suitable removal efficiency.

### 7. Comparison with other Adsorbents

The adsorbent prepared in this study was used to eliminate mercury from water sources, and the investigations showed the maximum removal percentage of 79.85% at pH 4 and  $q_m=1,058$  mg/g, predicted by Dubinin-Radushkevich isotherm. Table 7 provides information about the comparison between the adsorbent prepared in this study with other adsorbents in the literature. As can be seen, the prepared adsorbent in this study showed the highest  $q_m$  compared to other reported adsorbents.

## CONCLUSION

Due to the challenges posed by the incineration and disposal of polystyrene waste, a new method for reusing this waste has been proposed. Polystyrene was modified with chitosan and then functionalized with carbon disulfide, which was used as a novel adsorbent to remove mercury from aqueous media. FTIR analysis of the adsorbent was performed during the adsorbent synthesis to identify the functional groups on the modified adsorbent. BET and SEM analyses were performed to investigate the surface area and morphology of the prepared adsorbent, respectively. The adsorption process followed the Dubinin-Radushkevich isotherm, and the maximum removal percentage predicted in this isotherm was 79.85% at pH 4. The pseudo-second-order model was significantly more accurate than the pseudo-first-order model. It was observed that increasing contact time by up to 15 hours improved the adsorption capacity. However, this process slowed after 15 hours. Increasing the initial concentration resulted in an increase in the adsorption capacity of the prepared adsorbent, and the adsorbent was regenerated by washing with a hydrochloric acid solution with a concentration of 0.1 mol/L, showing that it can be reused at least three times.

## ACKNOWLEDGEMENT

This work was supported by the Department of Environmental Engineering, Graduate Faculty of Environment, University of Tehran, Tehran, Iran.

## SUPPORTING INFORMATION

Additional information as noted in the text. This information is available via the Internet at <http://www.springer.com/chemistry/journal/11814>.

## REFERENCES

1. S. Yadav, A. Yadav, N. Bagotia, A. K. Sharma and S. Kumar, *J. Water*

- Process Eng.*, **42**, 102148 (2021).
2. B. Sajjadi, R. M. Shrestha, W. Y. Chen, D. L. Mattern, N. Hammer, V. Raman and A. Dorris, *J. Water Process Eng.*, **39**, 101677 (2021).
3. H. F. Raad, A. Pardakhti and H. Kalarestaghi, *Pollution*, **7**, 395 (2021).
4. N. J. Langford and R. E. Ferner, *J. Hum. Hypertens.*, **13**, 651 (1999).
5. W.-T. Tsai, *Sustainability*, **14**, 1557 (2022).
6. F. Luo, J. L. Chen, L. L. Dang, W. N. Zhou, H. L. Lin, J. Q. Li, S. J. Liu and M. B. Luo, *J. Mater. Chem. A.*, **3**, 9616 (2015).
7. A. Prasetya, P. Prihutami, A. D. Warisaura, M. Fahrurrozi and H. T. B. Murti Petrus, *J. Environ. Chem. Eng.*, **8**, 103781 (2020).
8. M. Urgun-Demirtas, P. L. Benda, P. S. Gillenwater, M. C. Negri, H. Xiong and S. W. Snyder, *J. Hazard. Mater.*, **215-216**, 98 (2012).
9. S. M. Bachand, T. E. C. Kraus, D. Stern, Y. L. Liang, W. R. Horwath and P. A. M. Bachand, *Ecol. Eng.*, **134**, 26 (2019).
10. M. Negarestani, H. Farimaniraad, A. Mollahosseini, A. Kheradmand and H. Shayesteh, *Int. J. Phytoremediation*, **1** (2022).
11. Y. Wang, H. Li, Z. He, M. Zhang, J. Guan, K. Qian, J. Xu and J. Hu, *Environ. Sci. Pollut. Res. Int.*, **27**, 30254 (2020).
12. H. Prokkola, E. T. Nurmesniemi and U. Lassi, *ChemEngineering*, **4**, 51 (2020).
13. L. Duan, X. Hu, D. Sun, Y. Liu, Q. Guo, T. Zhang and B. Zhang, *Korean J. Chem. Eng.*, **37**, 1166 (2020).
14. M. Negarestani, A. Mollahosseini, H. Farimaniraad, H. Ghiasinejad, H. Shayesteh and A. Kheradmand, *Sep. Sci. Technol.*, **58**, 435 (2022).
15. A. Kheradmand, M. Negarestani, A. Mollahosseini, H. Shayesteh and H. Farimaniraad, *Sci. Rep.*, **12**, 16442 (2022).
16. P. Alipour Atmianlu, R. Badpa, V. Aghabalaei and M. Baghdadi, *J. Environ. Chem. Eng.*, **9**, 106514 (2021).
17. S. Armenise, W. SyieLuing, J. M. Ramirez-Velásquez, F. Launay, D. Wuebben, N. Ngadi, J. Rams and M. Muñoz, *J. Anal. Appl. Pyrol.*, **158**, 105265 (2021).
18. L. Li, J. Wang, C. Jia, Y. Lv and Y. Liu, *J. Water Process Eng.*, **39**, 101753 (2021).
19. J. Saleem, M. Adil Riaz and M. Gordon, *J. Hazard. Mater.*, **341**, 424 (2021).
20. M. Janmohammadi, M. Baghdadi, T. M. Adyel and N. Mehrdadi, *Sci. Total Environ.*, **752**, 141850 (2021).
21. I. Baker, *Fifty Mater. That Make World.*, **1** (2018).
22. J. Mao, W. Jiang, J. Gu, S. Zhou, Y. Lu and T. Xie, *Appl. Surf. Sci.*, **317**, 787 (2014).
23. N. C. F. Machado, L. A. M. de Jesus, P. S. Pinto, F. G. F. de Paula, M. O. Alves, K. H. A. Mendes, R. V. Mambri, D. Barrreda, V. Rocha, R. Santamaría, J. P. C. Trigueiro, R. L. Lavall and P. F. R. Ortega, *J. Clean. Prod.*, **313**, 127903 (2021).
24. Y. Pu, Z. Xie, H. Ye and W. Shi, *Water Sci. Technol.*, **83**, 2192 (2021).
25. A. L. Andraday and M. A. Neal, *Philos. Trans. R. Soc. B Biol. Sci.*, **364**, 1977 (2009).
26. C. Yu, W. Lin, J. Jiang, Z. Jing, P. Hong and Y. Li, *RSC Adv.*, **9**, 37759 (2019).
27. G. Liu, S. Wen, Y. Wang, J. Zhang, S. Huang and A. Chen, *Chem. Eng. Sci.*, **249**, 117331 (2022).
28. H. K. No and S. P. Meyers, *Rev. Environ. Contam. Toxicol.*, **163**, 1 (2000).
29. S. Olivera, H. B. Muralidhara, K. Venkatesh, V. K. Guna, K. Gopal

- akrishna and Y. Kumar K., *Carbohydr. Polym.*, **153**, 600 (2016).
30. M. V. Tsurkan, A. Voronkina, Y. Khrunyk, M. Wysokowski, I. Petrenko and H. Ehrlich, *Carbohydr. Polym.*, **252**, 117204 (2021).
31. R. Vajdi, N. Alvand, M. Baghdadi and G. N. Bidhendi, *J. Water Process Eng.*, **40**, 101898 (2021).
32. N. Ahmad, S. Sultana, M. Z. Khan and S. Sabir, *Chitosan based nanocomposites as efficient adsorbents for water treatment BT - modern age waste water problems?: Solutions using applied nanotechnology*, in: M. Oves, M. O. Ansari, M. Zain Khan, M. Shahadat, I. M. I. Ismail (Eds.), Springer International Publishing, Cham, 69 (2020).
33. H. Zeng, Y. Yu, F. Wang, J. Zhang and D. Li, *Colloids Surf. A Physicochem. Eng. Asp.*, **585**, 124036 (2020).
34. P. S. Bakshi, D. Selvakumar, K. Kadirvelu and N. S. Kumar, *Int. J. Biol. Macromol.*, **150**, 1072 (2020).
35. F. S. Al-Mubaddel, S. Haider, M. O. Aijaz, A. Haider, T. Kamal, W. A. Almasry, M. Javid and S. U.-D. Khan, *Polym. Bull.*, **74**, 1535 (2017).
36. M. Keshvardoostchokami, M. Majidi, A. Zamani and B. Liu, *Carbohydr. Polym.*, **273**, 118625 (2021).
37. A. Chen, C. Shang, J. Shao, Y. Lin, S. Luo, J. Zhang, H. Huang, M. Lei and Q. Zeng, *Carbohydr. Polym.*, **155**, 19 (2017).
38. J. Yang, Y. Han, Z. Sun, X. Zhao, F. Chen, T. Wu and Y. Jiang, *ACS Omega*, **6**, 15885 (2021).
39. Q. Wang, C. Zheng, Z. Shen, Q. Lu, C. He, T. C. Zhang and J. Liu, *Chem. Eng. J.*, **359**, 265 (2019).
40. A. C. Alavarse, E. C. G. Frachini, R. L. C. G. da Silva, V. H. Lima, A. Shavandi and D. F. S. Petri, *Int. J. Biol. Macromol.*, **202**, 558 (2022).
41. F. Doustdar, A. Olad and M. Ghorbani, *Int. J. Biol. Macromol.*, **208**, 912 (2022).
42. B. Gulen and P. Demircivi, *J. Mol. Struct.*, **1206**, 127659 (2020).
43. C.-H. Kuo, Y.-C. Liu, C.-M. J. Chang, J.-H. Chen, C. Chang and C.-J. Shieh, *Carbohydr. Polym.*, **87**, 2538 (2012).
44. J. Liu, W. Liu, Y. Wang, M. Xu and B. Wang, *Appl. Surf. Sci.*, **367**, 327 (2016).
45. S. Kamari, F. Ghorbani and A. M. Sanati, *Sust. Chem. Pharm.*, **13**, 100153 (2019).
46. B. Wang, J. Xia, L. Mei, L. Wang and Q. Zhang, *ACS Sust. Chem. Eng.*, **6**, 1343 (2018).
47. M. Baghdadi, *J. Environ. Chem. Eng.*, **5**, 1906 (2017).
48. A. Rezk, G. Gediz Ilis and H. Demir, *Therm. Sci. Eng. Prog.*, **34**, 101429 (2022).
49. M. D. Mullassery, N. B. Fernandez and T. S. Anirudhan, *Sep. Sci. Technol.*, **49**, 1259 (2014).
50. K. Johari, N. Saman, S. T. Song, J. Y. Y. Heng and H. Mat, *Chem. Eng. Commun.*, **201**, 1198 (2014).
51. H. Cui, Y. Qian, Q. Li, Q. Zhang and J. Zhai, *Chem. Eng. J.*, **211-212**, 216 (2012).
52. W. Du, L. Yin, Y. Zhuo, Q. Xu, L. Zhang and C. Chen, *Ind. Eng. Chem. Res.*, **53**, 582 (2014).